AD-A062 463 SOUTHERN METHODIST UNIV DALLAS TEX DEPT OF ELECTRICA--ETC F/G 9/3
ADAPTIVE DEMODULATION OF DIGITAL MODULATED SIGNALS.(U)
NOV 78 M D SRINATH N00014-76-C-0456
UNCLASSIFIED NL

| OF |
AD
A062463

END
DATE
FILMED
3-79
DDC

Unclassified

SECURITY CLASSIFICATION OF THIS PAGE (When Data Entered)

(12) LEVEL II

REPORT DOCUMENTATION PAGE		READ INSTRUCTIONS BEFORE COMPLETING FORM
1. REPORT NUMBER 1	2. GOVT ACCESSION NO.	3. RECIPIENT'S CATALOG NUMBER
4. TITLE (and Subtitle) (6) Adaptive Demodulation of Digital Modulated Signals,		5. TYPE OF REPORT & PERIOD COVERED Final Report, Jun 1977-Sept 78
		6. PERFORMING ORG. REPORT NUMBER
7. AUTHOR(s) (10) M. D. Srinath		8. CONTRACT OR GRANT NUMBER(s) (15) N00014-76-C-0456
9. PERFORMING ORGANIZATION NAME AND ADDRESS Department of Electrical Engineering, Southern Methodist University, Dallas, TX 75275		10. PROGRAM ELEMENT, PROJECT, TASK AREA & WORK UNIT NUMBERS NR 042-382/4-26-77
11. CONTROLLING OFFICE NAME AND ADDRESS Office of Naval Research, Department of the Navy, Arlington, VA 22217 (11) 34		12. REPORT DATE November 30, 1978
		13. NUMBER OF PAGES 34
14. MONITORING AGENCY NAME & ADDRESS (if different from Controlling Office) (9) Rept. no. 1 (Final) Jun 77 - Sep 78		15. SECURITY CLASS. (of this report) Unclassified
		15a. DECLASSIFICATION/DOWNGRADING SCHEDULE

16. DISTRIBUTION STATEMENT (of this Report)

Approved for Public release; distribution unlimited (12) 38p.

17. DISTRIBUTION STATEMENT (of the abstract entered in Block 20, if different from Report)

DDC RECEIVED DEC 20 1978 B

18. SUPPLEMENTARY NOTES

19. KEY WORDS (Continue on reverse side if necessary and identify by block number)

Autoregressive Models, Spectral Estimation, Identification, Digital Modulated Signals

20. ABSTRACT (Continue on reverse side if necessary and identify by block number)

The estimation of the frequency spectrum of signals is of widespread importance in such diverse areas as seismic signal processing, vibration measurements, biomedical signal processing, speech transmission, etc. In communication systems, the estimation of the spectrum of a signal is of importance for both demodulation of angle modulated signals and in frequency synchronization. A commonly used technique for spectral estimation in stochastic signals is to identify the parameters of an autoregressive model of the signal and then de-

next page

78 12 11 163

DD FORM 1 JAN 73 1473 EDITION OF 1 NOV 65 IS OBSOLETE

Unclassified

SECURITY CLASSIFICATION OF THIS PAGE (When Data Entered)

AD A062463

DDC FILE COPY

408 600

LB

termine the spectrum in terms of these parameters. Instead of idenfiying the autoregressive parameters, alternative parameters may be formulated which are preferable from an identification viewpoint. In this investigation, one such set of parameters is determined on the basis of sensitivity studies. The parameters are obtained from a nonlinear transformation of the autoregressive parameters. A maximum likelihood estimation scheme is used to obtain appropriate sequential algorithms for identification of these parameters. Several simulation examples are presented to illustrate the applicability of the algorithms for spectral estimation in a stationary stochastic process. In addition two examples in communication systems are presented to illustrate the applicability of the technique. The first is concerned with identifying an emitter by means of its spectral characteristics and involves adaptively determining the instantaneous frequency in the signal. The second example is in PN code acquisition in a frequency hopping spread spectrum system and illustrates the computational savings achieveable over other comparable methods presented in the literature.

ABSTRACT

The estimation of the frequency spectrum of signals is of widespread importance in such diverse areas as seismic signal processing, vibration measurements, biomedical signal processing, speech transmission, etc. In communication systems, the estimation of the spectrum of a signal is of importance for both demodulation of angle modulated signals and in frequency synchronization. A commonly used technique for spectral estimation in stochastic signals is to identify the parameters of an autoregressive model of the signal and then determine the spectrum in terms of these parameters. Instead of identifying the autoregressive parameters, alternative parameters may be formulated which are preferable from an identification viewpoint. In this investigation, one such set of parameters is determined on the basis of sensitivity studies. The parameters are obtained from a nonlinear transformation of the autoregressive parameters. A maximum likelihood estimation scheme is used to obtain appropriate sequential algorithms for identification of these parameters. Several simulation examples are presented to illustrate the applicability of the algorithms for spectral estimation in a stationary stochastic process. In addition two examples in communication systems are presented to illustrate the applicability of the technique. The first is concerned with identifying an emitter by means of its spectral characteristics and involves adaptively determining the instantaneous frequency in the signal. The second example is in PN code acquisition in a frequency hopping spread spectrum system and illustrates the computational savings achieveable over other comparable methods presented in the literature.

ADAPTIVE DEMODULATION OF DIGITAL MODULATED SIGNALS

Final Report

Prepared under ONR Contract NR 042-382

for

Office of Naval Research

Department of the Navy

Arlington, VA 22217

by

M. D. Srinath

Principal Investigator

Department of Electrical Engineering

Southern Methodist University

Dallas, TX 75275

1. Introduction:

Interest in the area of estimation of the frequency spectrum of signals has grown significantly in recent years. Estimation of the frequency spectrum has found wide applications in seismic signal processing, biomedical signal processing, speech transmission, analysis of Doppler radar returns, vibration measurements, etc. A variety of Fourier transforms methods have been developed for spectral estimation. An alternate technique for spectrum estimation is to fit an autoregressive (AR) or autoregressive moving average (ARMA) model to the process. For a signal modeled by the AR process

$$y(k) = \sum_{n=1}^{N} \alpha_n y(k-n) + w(k) \tag{1}$$

where $w(\cdot)$ is assumed to be a zero mean, Gaussian white process with variance V_w, the spectrum is given by

$$\Phi_y(\omega) = \left| \frac{1}{1-\sum_{n=1}^{N} \alpha_n e^{-j\omega n}} \right|^2 V_w \tag{2}$$

so that the problem of spectrum estimation becomes one of identifying the parameters of an AR model of the process.

Several techniques are available for the estimation of the parameters in a general AR model of the form of Eq. (1). The techniques basically require the solution of a set of equations involving the autocorrelation coefficients and require batch-processing of the data. In such techniques, the computation of the correlation coefficients constitues a substantial part of the total computational effort in obtaining the autore-

gressive parameters.

In many applications, the signal is not truly stationary and the spectral content of the signal may be varying. Typical examples are in speech or image processing or in communications. The short-time spectrum of a speech signal varies from interval to interval, so that the parameters of the associated AR model must be recomputed periodically. In image processing, the image intensity will not be the same over the entire picture. Thus, if an AR model is used to describe the image, the parameters of this model will not be constant over the entire image. In communication systems involving frequency or phase-modulation, the waveforms are typically characterized as having a narrowband time-varying spectrum. Demodulation then essentially requires estimating the instantaneous frequency in the spectrum of the received signal. Again, in spread spectrum systems involving frequency hopping, the receiver is required to determine the instantaneous frequency in the received signal. In all these cases, we therefore need to track the coefficients of the AR model adaptively in order to be able to estimate the spectrum of the signal.

It is clear from Eq. (1) that once the AR coefficients $\{\alpha_n\}$ have been identified, the short-term spectrum of the signal $y(\cdot)$ can be determined from Eq. (2). However, from the point of view of estimating the signal spectrum, the parameters $\{\alpha_n\}$ of the autoregressive model may not be the best set for identification. Recent investigations have shown that alternative coefficients can be associated with the AR model which, for a given data length, can lead to better spectral estimation. One such set of coefficients is the partial correlation coefficients [1,2].

The present research has been concerned with determining other sets

of coefficients which may lead to better spectral estimation and to obtain algorithms for the identification of these parameters. Alternative coefficients have been determined which seem to provide better estimates of the short-time spectrum using finite length data. In the next section we formulate a set of such coefficients and illustrate the use of autoregressive spectral estimation techniques in two communications examples.

2. Alternative Coefficients:

We now consider the problem of formulating alternative coefficients associated with the model of Eq. (1). Let us denote by $\underset{\sim}{\theta}$ the (as yet undersignated) parameter vector to be identified. Let Y_k denote the set of observations $\{y(1), y(2) \ldots y(k)\}$. If we characterize $\underset{\sim}{\theta}$ as a nonrandom parameter, we can use the maximum likelihood (ML) technique for identification. The ML estimate of $\underset{\sim}{\theta}$ is obtained by maximizing the conditional density function $p(\underset{\sim}{Y}_k \mid \underset{\sim}{\theta})$. We note that

$$p(\underset{\sim}{Y}_k|\underset{\sim}{\theta}) = p(y(k)|\underset{\sim}{Y}_{k-1},\underset{\sim}{\theta})p(y(k-1)|\underset{\sim}{Y}_{k-2},\underset{\sim}{\theta}) \ldots p(y(0)) \tag{3}$$

so that the log-likelihood function is

$$\ell n\ p(\underset{\sim}{Y}_k|\underset{\sim}{\theta}) = \sum_{j=1}^{k} \ell n\ p(y(j)|\underset{\sim}{Y}_{j-1},\underset{\sim}{\theta}) \tag{4}$$

Because of the Gaussian assumptions on $w(\cdot)$, it easily follows that $y(j)$ is Gaussian. From Eq. (1), we can write

$$E\{y(j)|\underset{\sim}{Y}_{j-1},\underset{\sim}{\theta}\} = -\sum_{i=1}^{N} \alpha_i y(j-i)$$

$$\mathrm{var}\{y(j)|\underset{\sim}{Y}_{j-1},\underset{\sim}{\theta}\} = \mathrm{var}\{w(j)\} = V_w$$

The log-likelihood function therefore is

$$\ln p(\underset{\sim}{Y}_k | \underset{\sim}{\theta}) = -\frac{k}{2} \ln(2\pi V_w) - \frac{1}{2V_w} \sum_{j=1}^{k} [y(j) - \sum_{i=1}^{N} \alpha_i y(j-i)]^2 \tag{5}$$

The maximum likelihood estimate of $\underset{\sim}{\theta}$ is thus that value of $\underset{\sim}{\theta}$ which minimizes the quantity $\sum_{j=1}^{k} [y(j) - \sum_{i=1}^{N} \alpha_i y(j-i)]^2$. If we define $\varepsilon(j)$ as the residual,

$$\varepsilon(j) = y(j) - \sum_{i=1}^{N} \alpha_i y(j-i) \tag{6}$$

it is clear that $\varepsilon(\cdot)$ represents the output of a linear system with transfer function $H(z^{-1}) = 1 - \sum_{i=1}^{N} \alpha_i z^{-i}$ and input $y(\cdot)$. The ML estimate $\hat{\underset{\sim}{\theta}}$ can then be obtained by choosing the parameters of this system such that the square sum of its output is minimized.

The preceding discussion gives us a basis for associating a set of parameters with an AR process. We can obtain realizations of the transfer function $H(z^{-1})$ using different parameter sets. Since the identification of the parameters involves minimizing the square sum of the corresponding outputs, we can compare these parameter sets from an identification viewpoint by considering the sensitivity of the output to variations in the parameters. If the sensitivity is low, the residual is not affected as much by variations in the parameter. This implies that even if the parameters are not identified very accurately, $H(z^{-1})$ and hence $\Phi_y(\omega)$ can be estimated well. Hence for a given data length the parameter set with lower sensitivity should yield a better spectral estimate.

One method of comparing different realizations of $H(z^{-1})$ is to use a time-domain sensitivity function defined as follows [3]. Let "a" denote a parameter in the system and $s(k,a)$ the corresponding output at the k^{th} stage. Then the sensitivity function of $s(.,.)$ with respect to "a" is defined as

$$S_a^s(k) = \frac{\partial \ln s(k,a)}{\partial \ln a}$$

$$= \frac{\partial s(k,a)}{\partial a} \cdot \frac{a}{s(k,a)} \tag{7}$$

Equation (7) represents the percentage change in the output $s(k,a)$ due to small perturbations in the values of a. It is easy to see from Eq. (7) that the sensitivity function $S_a^s(k)$ is completely determined if the gradient vector $\frac{\partial s}{\partial a}$ can be computed. This can be easily done by using sensitivity models [3,4].

Consider the linear system shown in Figure 1 in which it is desired to find the sensitivity of the output $s(k)$ with respect to variations in the parameter "a". If $e_2(k)$ is added to the output of the gain element "a" in the model, every signal in the model (except the output of "a") is the partial derivative with respect to "a" of the corresponding signal in the system. This can be seen by considering the equations of the system. From Figure 1

$$e_2(k) = \sum_{j=0}^{k} w_{12}(k-j)\ u(j) + \sum_{j=0}^{k} w_{32}(k-j)\ e_3(j) + e_2(0)$$

$$e_3(k) = ae_2(k)$$

$$e_4(k) = s(k) = \sum_{j=0}^{k} w_{14}(k-j)\ u(j) + \sum_{j=0}^{k} w_{34}(k-j) e_3(j) + e_4(0) \tag{8}$$

where w_{ij} represents the system weighting function between the input node i and output node j with the output of "a" open-circuited. Partial differentiation of the above equations with respect to "a" yields

$$
\begin{aligned}
\frac{\partial e_2(k)}{\partial a} &= \sum_{j=0}^{k} w_{32}(k-j)\ \frac{\partial e_3(j)}{\partial a} \\
\frac{\partial e_3(k)}{\partial a} &= a\ \frac{\partial e_2(k)}{\partial a} + e_2(k) \qquad (9) \\
\frac{\partial s(k)}{\partial a} &= \sum_{j=0}^{k} w_{34}(k-j)\ \frac{\partial e_3(j)}{\partial a}
\end{aligned}
$$

Thus the gradients are obtained as the outputs from the exact model with zero input and $e_2(k)$ fed at the output of the gain element "a".

When the sensitivity with respect to several parameters is needed, it is necessary to use as many models as parameters. If the outputs of these parameters end at a common summing junction however, all the sensitivity functions can is determined simultaneously by the use of a single model

3. Choice of Parameter Set for Identification

We now consider various realizations of the transfer function $H(z^{-1})$ in terms of different parameter sets and investigate their sensitivity properties with a view to determining the best set for identification.

As indicated earlier, one set of coefficients is the partial correlation coefficients. The partial correlation coefficient p_n, n = 1 ... N are obtained from the AR parameters α_i by the following set of recursions: For n = N,N-1 ..., 1

$$a_i^{n-1} = \frac{1}{1 - p_n^2} [a_i^n - p_n a_{n-i}^n] \qquad i = 1,2 \ldots n-1$$

$$a_0^{n-1} = a_o^n = 1$$

$$p_n = a_{n-1}^{n-1}$$

with $a_i^N = \alpha_i \qquad i = 1,2 \ldots N$

$$p_N = \alpha_N \tag{10}$$

To obtain a realization in terms of these parameters, let us define the polynomials

$$F_n(z^{-1}) = \sum_{i=0}^{n} a_i^n z^{-i}, \qquad n = s, s-1, \ldots, 1 \tag{11a}$$

and

$$G_n(z^{-1}) = \sum_{i=0}^{n} a_{n-i}^n z^{-i} \tag{11b}$$

Now Eq. (10) can be rewritten as

$$a_i^n = a_i^{n-1} + p_n a_{n-i}^{n-1} \qquad i = 1, \ldots, n-1 \tag{12}$$

It then follows by direct substitution of Eq. (12) in Eq. (11a) and Eq. (11b) that

$$F_n(z^{-1}) = F_{n-1}(z^{-1}) + p_n G_{n-1}(z^{-1}) \tag{13}$$

and

$$zG_n(z^{-1}) = G_{n-1}(z^{-1}) + p_n F_{n-1}(z^{-1}) \tag{14}$$

For any input X(z) therefore, we can determine the output of the system with transfer function $F_n(z^{-1})$ in terms of the outputs $F_{n-1}(z^{-1})X(z)$ and

$G_{n-1}(z^{-1})X(z)$ by use of Eqs. (13 and (14). Recursive use of these equations then yields the lattice realization of Fig. 2 for the all zero transfer function $H(z^{-1})$. The initial values for starting the recursion are

$$F_0(z^{-1}) = 1 \text{ and } G_0(z^{-1}) = z^{-1}$$

The coefficients p_n have also been referred to as reflection coefficients. The name comes from transmission line theory in which p_n is considered as the reflection coefficient at the boundary between two sections of transmission line with characteristic impedances Z_n and Z_{n+1}. p_n is then given by

$$p_n = \frac{Z_{n+1} - Z_n}{Z_{n+1} + Z_n} \qquad 1 \leq n \leq N \tag{15}$$

The transfer function $H(z^{-1})$ can then be considered as that of a sequence of these sections with impedance ratios given by

$$\frac{Z_{n+1}}{Z_n} = \frac{1 + p_n}{1 - p_n} \qquad 1 \leq n \leq N \tag{16}$$

The same phenomenon holds for any type of situation where there is a plane wave transmission with normal incidence on sections with different impedances. For example, for the case of an acoustic tube with n sections of varying cross-sections, the impedance ratios reduce to the inverse ratio of the consecutive cross-sectional areas. An example is the acoustical tube model of the vocal tract used in speech processing applications [5]. We can use as a second set of parameters to be used in spectral estimation, the set $\{S_n\}$ defined as

$$S_n = \frac{1 - p_n}{1 + p_n} \qquad n = 1,2 \ldots N \tag{17}$$

In order to obtain a realization of $H(z^{-1})$ in terms of $\{S_n\}$, we substitute Eq. (17) into Eqs. (13) and (14) to obtain

$$(1 + S_n)\, F_n(z^{-1}) = (1 + S_n)\, F_{n-1}(z^{-1}) + (1 - S_n)\, G_{n-1}(z^{-1}) \tag{18}$$

$$(1 + S_n)\, G_n(z^{-1}) = z^{-1} \left[(1 + S_n)\, G_{n-1}(z^{-1}) + (1 - S_n)\, F_{n-1}(z^{-1}) \right] \tag{19}$$

One stage of the realization is shown in Figure 3.

In order to compare the two parameter sets with regard to their sensitivity properties, we use sensitivity models as discussed in the previous section. The sensitivity model for the parameters $\{p_n\}$ is shown in Figure 4. A similar model can be obtained for the parameters $\{S_n\}$ also [6].

In order to compare the two structures to determine which is less sensitive, we use as a measure of sensitivity, the following:

$$J = \frac{1}{k_f} \sum_{k=0}^{k=k_f} \sum_{i=1}^{N} \left|\left| S^s_{\alpha_i}(k) \right|\right|^2 \tag{20}$$

It is easy to verify that the time-domain sensitivity measure defined by Eq. (20) is equivalent to the frequency domain sensitivity measure defined in [7] , as

$$\frac{\partial s}{\partial p_i} = \lim_{\Delta k_i \to 0} \left| \frac{1}{\Delta k_i} \left[\frac{1}{2\pi} \int_{-\pi}^{\pi} \left| \log \Phi_y(d_i,\omega) - \log \Phi_y(d_i + \Delta d_i,\omega) \right| d\omega \right] \right| \tag{21}$$

where $\Phi_y(\cdot,\omega)$ is the spectrum of the signal $y(\cdot)$ [see Eq. (2)], and the quantity in brackets is the spectral deviation due to a perturbation in the i^{th} coefficient.

Several examples were run to compare the sensitivities of the two realizations. We present here a typical example in which $H(z^{-1})$ was chosen as

$$H(z^{-1}) = 1 - 2.8775\, z^{-1} + 2.5673\, z^{-2} - .7897\, z^{-3}$$

The corresponding parameters obtained from Eqs. (10) and (17) are

$$p_1 = 0.9657, \quad p_2 = 0.7820, \quad p_3 = 0.2683$$

$$S_1 = 0.0175, \quad S_2 = 0.1223, \quad S_3 = 0.5825$$

Figures 5 and 6 show the sensitivities with respect to the two sets of parameters when the input to the sensitivity model is a unit step input. As can be seen, the sensitivities with respect to the parameters $\{S_n\}$ are less than with respect to the $\{p_n\}$. This is also illustrated in Table I which shows the sensitivity measure of Eq. (20) for the example. In general, the examples show that when the zeros of $H(z^{-1})$ are close to the unit circle, the sensitivity with respect to $\{S_n\}$ is better than with respect to $\{p_n\}$.

While the discussions above show that a realization of $H(z^{-1})$ using the $\{S_n\}$ parameters does indeed exhibit lower sensitivity, these coefficients are not really suitable from an identification viewpoint since some of the nice symmetry properties associated with the $\{p_n\}$ parameters no longer hold. For example, p_n in the range $(-1,0)$ yields a value for S_n in $(1,\infty)$, whereas p_n in $(0,1)$ corresponds to S_n in $(0,1)$, so that the range of S_n is $(0,\infty)$. However, if we define the coefficients L_n as

$$L_n = \log S_n \qquad n = 1, \ldots N \tag{22}$$

it is clear that we will retain the symmetry properties of $\{p_n\}$ while obtaining lower sensitivity. For these reasons, the parameter vector $\underset{\sim}{\theta}$ was chosen to be

$$\underset{\sim}{\theta} = [\ L_1\ L_2\ \ldots\ L_N\ ]^T$$

where N defines the order of the model.

4. Identification Algorithm

We now consider the estimation of the parameters L_n. In order to obtain the maximum likelihood estimates $\hat{L}_n$, we follow the procedure in [4] and minimize the output $\varepsilon(\cdot)$ of the system with transfer-function $H(z^{-1}) = 1 - \sum_{i=1}^{N} \alpha_i z^{-i}$. We use a realization of this transfer function in terms of the parameters $\{L_n\}$ obtained by substituting Eq. (22) into Eqs. (18) and (19) and seek an estimate $\{\hat{L}_n\}$ such that the square sum of the output is minimized. The realization is shown in Figure 7. From the figure, the equations describing the realization can be written down as

$$\varepsilon_f^{n+1}(k) = \varepsilon_f^n(k) + \frac{1-e^{L_{n+1}}}{1+e^{L_{n+1}}}\ \varepsilon_b^n(k-1) \tag{23}$$

$$n = 1, 2, \ldots, N$$

$$\varepsilon_b^{n+1}(k) = \varepsilon_b^n(k-1) + \frac{1-e^{L_{n+1}}}{1+e^{L_{n+1}}}\ \varepsilon_f^n(k) \tag{24}$$

with $\varepsilon_f^o(k) = \varepsilon_b^o(k) = y(k)$. The estimate $\hat{L}_{n+1}$ obtained by minimizing the square sum of the residuals $\{\varepsilon_f^{n+1}(\cdot)\}$ are given by

$$\hat{L}^f_{n+1}(k) = \ln \left[\frac{\sum_{i=1}^{k} \left[\varepsilon^n_f(i)\varepsilon^n_b(i-1)+\{\varepsilon^n_b(i-1)\}^2 \right]}{\sum_{i=1}^{k} \left[\{\varepsilon^n_b(i-1)\}^2-\varepsilon^n_f(i)\varepsilon^n_b(i-1) \right]} \right] \tag{25}$$

where ^ refers to estimated values.

Minimizing $\{\varepsilon^{n+1}_b(\cdot)\}$ similarly yields

$$\hat{L}^b_{n+1}(k) = \ln \left[\frac{\sum_{i=1}^{k} \left[\varepsilon^n_f(i)\varepsilon^n_b(i-1)+\{\varepsilon^n_f(i)\}^2 \right]}{\sum_{i=1}^{k} \left[\{\varepsilon^n_f(i)\}^2-\varepsilon^n_f(i)\varepsilon^n_b(i-1) \right]} \right] \tag{26}$$

Since the output y(k) is assumed to be stationary, it can be shown by direct computation that for large values of k, $\sum_{i=1}^{k} \{\varepsilon^n_b(i-1)\}^2 = \sum_{i=1}^{k} \{\varepsilon^n_f(i)\}^2$.

We can then combine Eqs. (25) and (26) to get

$$\hat{L}_{n+1}(k) = \ln \left[\frac{\sum_{i=1}^{k} \{\varepsilon^n_f(i)+\varepsilon^n_b(i-1)\}^2}{\sum_{i=1}^{k} \{\varepsilon^n_f(i)-\varepsilon^n_b(i-1)\}^2} \right] \tag{27}$$

Equation (26) can be put into sequential form to yield

$$\hat{L}_{n+1}(k) = \hat{L}_{n+1}(k-1) + \ln \left[1 + \frac{\{\varepsilon^n_f(k)+\varepsilon^n_b(k-1)\}^2}{\sum_{i=1}^{k-1} \{\varepsilon^n_f(i)+\varepsilon^n_b(i-1)\}^2} \right] - \ln \left[1 + \frac{\{\varepsilon^n_f(k)-\varepsilon^n_b(k-1)\}^2}{\sum_{i=1}^{k-1} \{\varepsilon^n_f(i)-\varepsilon^n_b(i-1)\}^2} \right] \tag{28}$$

Equations (23), (24) and (28) constitute a complete set of algorithms for identifying the parameters $\{L_n\}$.

5. Simulation Examples

Several examples were simulated to illustrate the use of the identification algorithm. These results are summarized in Table II. Example 1 is an AR process with real poles at 0.9 and -0.9. The estimated parameters are within one percent. Example 2 is an AR process with a pair of complex poles at a radius of 0.95 and the estimated parameters are within 2.32 percent. Examples 3 and 4 are AR processes with 4 real poles. Note that the percentage error in the last estimated parameter becomes larger as the poles approach the unit circle. Examples 5 to 7 are AR processes with complex poles. As before, the errors tend to increase as the poles approach the unit circle. In every case a data length of 5000 samples was used. The initial estimates of the parameter were chosen as zero.

The estimate of the spectrum $\Phi_y(\omega)$ can be obtained from Eq (2). In order to directly relate the spectrum to the parameters $\{L_n\}$, we can use a realization of the transfer function

$$G(\omega) = \frac{1}{1-\sum_{n=1}^{N} \alpha_n e^{-j\omega n}} \tag{29}$$

in terms of these parameters, as shown in Fig. 8 [9]. This realization is obtained from Fig. 7 by reversing the direction of signal flow. A typical example is shown in Fig. 9 which plots the true and estimated spectra for Example 6 in Table II. As can be seen from the figure, the estimate follows the true spectrum closely.

In addition, two typical examples of spectral estimation in communication systems were investigated. The first example involved identifying

emitters by their spectral characteristics. The problem is to determine the instantaneous frequency of the largest amplitude sinusoid within the portion of the spectrum of interest [10]. The model is assumed to consist of a single large-amplitude sinusoid (the signal) plus a number of smaller amplitude sinusoid (interference). The observations were assumed to be corrupted by additive noise n(k).

The data was generated using the following model:

$$x(k) = 1000 \cos(\theta_1(k)) + 100 \cos(\theta_2(k)) + n(k), \quad k = 0,1,2, \ldots, 511$$

where

$$\theta_1(k) = 340\, \pi\, k\Delta t - 24 \cos(\tfrac{5\pi}{2}\, k\Delta t - \tfrac{\pi}{2}) + 2$$

$$\theta_2(k) = 320\, \pi\, k\Delta t - 40 \cos(2\pi\, k\Delta t) - 2$$

$$\Delta t = 0.00125$$

It is desired to determine the instantaneous frequency every 0.04 sec, where L the instantaneous frequency is defined as $\frac{1}{2\pi} \frac{d\Phi}{dt}$ and Φ is the argument of the sinusoid. The noise n(k) is a sequence of pseudo-uniformly distributed random numbers in the range $-100 \leq n(k) \leq 100$. The spectrum of interest is in the range from 130 to 270 Hertz. The sampling rate was chosen to be 800 samples/sec.

The power spectrum was estimated for every 32 samples. The estimation algorithm was used repeatedly on the same set of data points till convergence was obtained. At each iteration the last estimated value from the previous estimate was used as the initial estimate. It was found that while the algorithms had to be iteratively applied 30 times over the

first data set of 32 samples, only 4 iterations were required for subsequent intervals to achieve reasonable convergence of the estimates. The results are tabulated in Table III for model orders 2,4 and 6.

The second communication example was taken from spread spectrum systems. Spread spectrum systems have found increasing applicability in areas such as remote piloted vehicles, anti-jam systems, packet radio network, multiple-access systems, etc. A spread spectrum signal is generated by modulating a data signal onto a wide band carrier so that the resultant transmitted signal has bandwidth much larger than the data signal. In the frequency hopping (FH) spread spectrum system an n-stage PN sequence generator is used to determine the carrier frequency over each signalling interval (called a chip interval). The carrier is then modulated by the data before transmission. At the receiver, the signal is demodulated by correlating it with a signal generated locally. For proper demodulation, the frequency of the local signal must be the same as that of the carrier. It follows that a primary requirement in such receivers is to set the initial state and maintain the phase of the locally generated signal in synchronism with the received PN signal. In this example we consider the application of the spectral estimation technique discussed earlier to the problem of PN code acquisition at the receiver of a frequency hopping system [11]. For purposes of clarity we will assume that the data consists of a single bit over each chip interval.

A simple block diagram of an FH transmitter is shown in Figure 10. An n-stage linear feedback shift register generates a PN sequence of length 2^n-1. The output from the shift register stages is used as the binary input $b_n b_{n-1} \cdots b_2 b_1$ to a frequency synthesizer which generates a signal at

the frequency corresponding to the binary number $b_n b_{n-1} \dots b_1 b_0$, where b_0 is the data bit. The frequency hopping rate can be either equal to or a multiple of the data rate. We will assume here that the PN code bit rate is equal to the data bit rate. The synthesizer output is suitably amplified and upconverted to the required frequency for transmission. The transmitted signal can be expressed as

$$s(t) = \sqrt{2P} \sum_{k=-\infty}^{\infty} \cos(2\pi f_k t + \phi_k) \text{ rect } \left(\frac{t-kT}{T}\right)$$

where f_k is the hopped frequency corresponding to the (n+1)-bit binary number during the kth chip interval where each interval is of duration T. The phase ϕ_k is assumed to be uniformly distributed between 0 and 2π for non-coherent frequency synthesizers. The instantaneous spectrum of the transmitted signal thus is a single discrete line.

The operation of the FH receiver can be easily explained with the aid of the block diagram in Figure 11. A shift register is used to generate a replica of the PN sequence used at the transmitter. The n-bit binary number corresponding to the shift register state is used as input to the frequency synthesizer which generates one of the possible 2^n frequency signals. The received signal is appropriately down-converted and multiplied with the locally generated signal resulting in an intermediate frequency signal that is frequency shift keyed by the data, so that

$$r'(t) = A \sum_{k=-\infty}^{\infty} \cos(2\pi f_{IF} + 2\pi\Delta f_k + \Psi_k) \text{ rect}\left(\frac{t-kT}{T}\right) + n'(t)$$

where Δf_k corresponds to the kth data bit, and n'(t) represents the noise term. This signal is then demodulated by conventional techniques.

Before a meaningful FSK demodulation can be attempted, the locally generated PN sequence must be synchronized to the received sequence. This synchronization is a two-step process: initial acquisition and tracking.

It is clear from the previous example, that the identification algorithm presented in this report can be used to identify the instantaneous frequency in the spread signal and thus provide tracking. However, initial acquisition can be time consuming if a serial search is conducted over all possible phases of a long PN sequence. The problem of PN code acquisition at the receiver of a FH system is aimed at rapid acquisition of the initial state of the transmitter PN code generator. This initial state is used in the receiver PN code generator which is a hardware replica of the transmitter PN code generator. After PN code acquisition the receiver PN code generator is locked on to the FH receiver. One such PN code acquisition scheme ASEAT, Autoregressive Spectral Estimation Acquisition Technique is considered in [11]. The technique essentially consists of estimating n successive transmitted frequencies and hence n successive PN code generator states. The most significant bits (MSB) of these n successive PN code generator states are shifted into another shift register which at the end of this n stage operation will contain the initial PN code generator state to a high degree of accuracy. In effect this assumes the structure of the PN code generator to be a shift register with a feedback at the least significant bit. Thus the acquisition logic uses the MSB of the estimated PN state at each stage and hence acquisition time is of the order of nT seconds. If the estimated state is accurate to k most significant bits then the acquisition

logic can be modified to given an acquisition time of the order of $(n-k+1)T$ seconds.

The spectral estimation algorithm presented in the earlier sections of this report was applied to the problem of PN code acquisition in the FH system described above. For purposes of comparison with the results in [11], the system was simulated using a data rate of 10 Kbps and with $n = 9$. The number of hopping frequencies used was equal to 1022. The 9-stage PN-code generator is a maximal length sequence generator, generated by the primitive polynomial

$$P(x) = 1 + x^4 + x^9$$

The PN code generator is realized using a shift register and an exclusive or gate as shown in Fig. 11. The initial and successive states of the PN code generator at the transmitter are 406,300,89,179,359,207,414,316, 120,241, ... etc. The data bit is augumented as the least significant bit to the 9-bit PN generator state and the resulting number is used to generate the transmitted signal with one of the 1022 uniformly spaced frequencies lying in the interval $0.1\pi < \Omega_i < 0.78\pi$. The received signal is obtained by adding zero-mean white gaussian noise such that the carrier to noise ratio is -12db. The estimation algorithm is used to estimate the transmitted frequency and hence the state of the PN-generator.

The successive PN generator states and its estimates are summarized in Table IV. The estimates for model order 4 are comparable to the results in [11] which uses a model order 16 and hence a large reduction in model order is obtained. Since the acquisition logic in [11] uses only the MSB of the estimated state in each successive state, from Table V it can

be seen that even a model order of 2 can be used without any acquisition error, thus reducing the computational efforts considerably.

As suggested earlier the accuracy of the estimation scheme allows the use of more bits of each estimated state. Successive estimates of a particular bit of the initial state can be passed through a majority decoder to further reduce the error probability in the estimation of the initial state. An acquisition scheme using an estimator of model order 4, 6 most significant bits of the estimated state at each state and a majority 3 decoder for each bit of the initial state to be estimated is shown in Table V . The acquisition logic acquires the initial state to be 406 which in fact was the transmitted initial state. The lock-in time for the acquisition logic is 4T seconds as compared to 9T seconds for the acquisition logic in [11].

6. Conclusions

This report has considered the estimation of parameters in an autoregressive model of a stationary stochastic process. A set of parameters which are more suitable from an identification point of view were determined on the basis of sensitivity studies. The parameters are obtained from a nonlinear transformation of the autoregressive parameters. A maximum likelihood estimation scheme was used to obtain appropriate sequential algorithms for identification of these parameters. Several simulation examples are presented to illustrate the applicability of the algorithms for spectral estimation in a stationary stochastic process.

One of the original purposes of the investigation was to determine the applicability of the spectral estimation technique to the problem of

demodulation of digital modulated signals. With this in view two examples in communication systems were considered. The first was concerned with identifying an emitter by means of its spectral characteristics and involved adaptively determining the instantaneous frequency in the signal. The second example was in PN code acquisition in a frequency hopping spread spectrum system. The simulation results show the applicability of algorithms to this problem.

References

1. N. Levinson, "The Wiener RMS (Root Mean Square) Error Criterion in Filter Design and Prediction", J. Math. Phys. Vol. XXV, pp. 261-278 Jan. 1947.

2. E.A. Robinson, Multichannel Time Series Analysis with Digital Computer Programs, Holden-Day, San Francisco, CA., 1967.

3. R. Tomovic, Sensitivity Analysis of Dynamical Systems, McGraw-Hill Book Co., New York, 1963.

4. D.F. Wilkie and W.R. Perkins, "Generation of Sensitivity Functions for Linear Systems Using Low-Order Models," IEEE Trans. on Automatic Control, Vol. AC-14, No. 2, pp. 123-130, April 1969.

5. J.D. Markel and A.H. Gray, Jr., Linear Prediction of Speech, Springer-Verlag, 1976.

6. M.M. Viswanathan, "Digital Filter Structures and Application to Identification", Ph.D. Thesis, Southern Methodist University, Dallas, TX., 1975.

7. J. Makhoul and R. Viswanathan, "Quantization Properties of Transmission Parameters in Linear Predictive Systems," BBN Report No. 2800, Bolt Beranek and Newman, Inc., Cambridge, Mass., April, 1974.

8. M.D. Srinath and M.M. Viswanathan, "Sequential Algorithm for Identification of Parameters of an Autoregressive Process", IEEE Trans. Auto-Control, Vol. AC-20, No. 4, pp. 542-546, Aug. 1975.

9. M.D. Srinath, "Digital Filter Structures with Low Sensitivity", Final Report, NSF Grant GK-43463, Nov. 1976.

10. RADC Spectrum Estimation Workshop (Problems and Solutions), 24,25, & 26 May, 1978.

11. G.S. Takhar, A.K. El-Hakeem and S.C. Gupta, "Frequency Hopping Acquisition by Autoregressive Spectral Estimation", Proc ITC, Toronto, Canada, 1978.

TABLE I

COMPARISON OF SENSITIVITY MEASURES FOR DIFFERENT REALIZATIONS FOR THE EXAMPLE

Parameter	Sensitivity measure of each Parameter			Overall Sensitivity Measure
	1	2	3	
P_n	0.3536×10^{2}	0.7783×10^{1}	0.2197	0.4343×10^{2}
S_n	0.2783×10^{-2}	0.5642×10^{-1}	0.4777×10^{1}	0.4836×10^{1}

TABLE II

Example No.	Order of the AR process	Actual Location of Poles	Actual $\{L_i\}$	Estimated $\{L_i\}$ after 5000 samples
1	2	± 0.9	0.0	-0.0582994
			2.254058	2.2753185
2	2	$0.95e^{\pm j\frac{\pi}{4}}$	1.7590354	1.754843
			-2.9710717	-2.9023474
3	4	0.5	4.1404499	4.1142841
		0.55	-2.6003106	-2.6100783
		0.6	1.1321468	1.0957899
		0.65	-0.2153282	-0.1664129
4	4	0.8	7.4872535	7.5726943
		0.85	-5.7861546	-5.7197308
		0.9	3.8302774	3.4646811
		0.95	-1.32915	-0.476785
5	4	$0.7e^{\pm j\frac{\pi}{6}}$	2.6609324	2.6694032
		$0.5e^{\pm j\frac{\pi}{4}}$	-2.0607646	-2.0663978
			0.8972335	0.8581285
			-0.2462367	-0.2415095
6	4	$0.8e^{\pm j\frac{\pi}{6}}$	2.3307328	2.3447747
		$0.7e^{\pm j\frac{\pi}{3}}$	-2.2850604	-2.2834348
			1.165021	1.1353965
			-0.6490662	-0.6382545
7	4	$0.95e^{\pm j\frac{\pi}{4}}$	1.8227941	1.8224967
		$0.7e^{\pm j\frac{\pi}{4}}$	-4.1579523	-4.0788953
			1.5375355	1.528485
			-0.9499867	-0.892745

Table III

Time	Actual Instantaneous Frequency	Estimated Instantaneous Frequency		
		Model Order 2	Model Order 4	Model Order 6
0.04	141.47	140.63	140.63	143.75
0.08	145.73	155.47	150.78	148.44
0.12	152.37	150.78	150.78	150.78
0.16	160.73	156.25	152.34	151.56
0.20	170.00	166.41	170.31	169.53
0.24	179.27	176.56	176.56	175.78
0.28	187.63	174.22	178.91	178.13
0.32	194.27	198.44	198.44	197.66
0.36	198.53	200.78	200.78	200.78
0.40	200.00	200.78	200.78	200.78
0.44	198.53	200.78	200.78	200.00
0.48	194.27	200.00	200.00	200.00
0.52	187.63	194.53	194.53	195.31
0.56	179.27	182.03	179.69	179.69
0.60	170.00	175.00	175.00	175.78
0.64	160.73	174.22	168.75	169.53

Table IV

True PN-generator Content	Estimated PN-generator Content					
	Model Order 2	Model Order 3	Model Order 4	Model Order 5	Model Order 6	Model Order 7
406	401.13	407.00	407.73	406.26	407.00	407.00
300	301.32	300.59	300.59	300.59	300.59	300.59
89	100.25	93.64	90.70	89.97	89.24	89.97
179	187.57	180.24	178.77	180.24	179.50	179.50
359	357.10	361.50	359.30	360.03	360.03	360.03
207	213.99	207.39	207.39	208.12	207.39	208.12
414	408.47	415.07	415.80	414.34	415.07	415.07
316	316.00	317.47	316.73	316.73	316.73	316.73
120	131.80	122.99	120.79	120.06	120.79	120.79
241	244.82	239.68	242.61	241.15	241.88	241.88

Table V

True PN-generator Content in Decimal	True PN-generator Content in Binary	Estimated PN-generator Content with model order 4 in Decimal	Estimated PN-generator Content with model order 4 in Binary
406	1 1001 0110	408	1 1001 1000
300	1 0010 1100	301	1 0010 1101
89	0 0101 1001	91	0 0101 1011
179	0 1011 0011	179	0 1011 0011

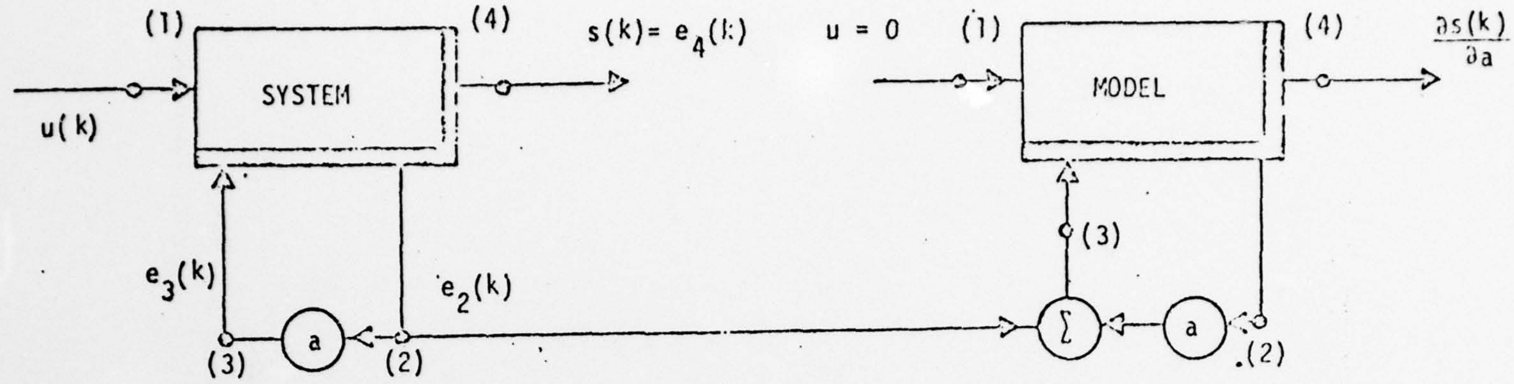

FIG. 1: SENSITIVITY MODELS

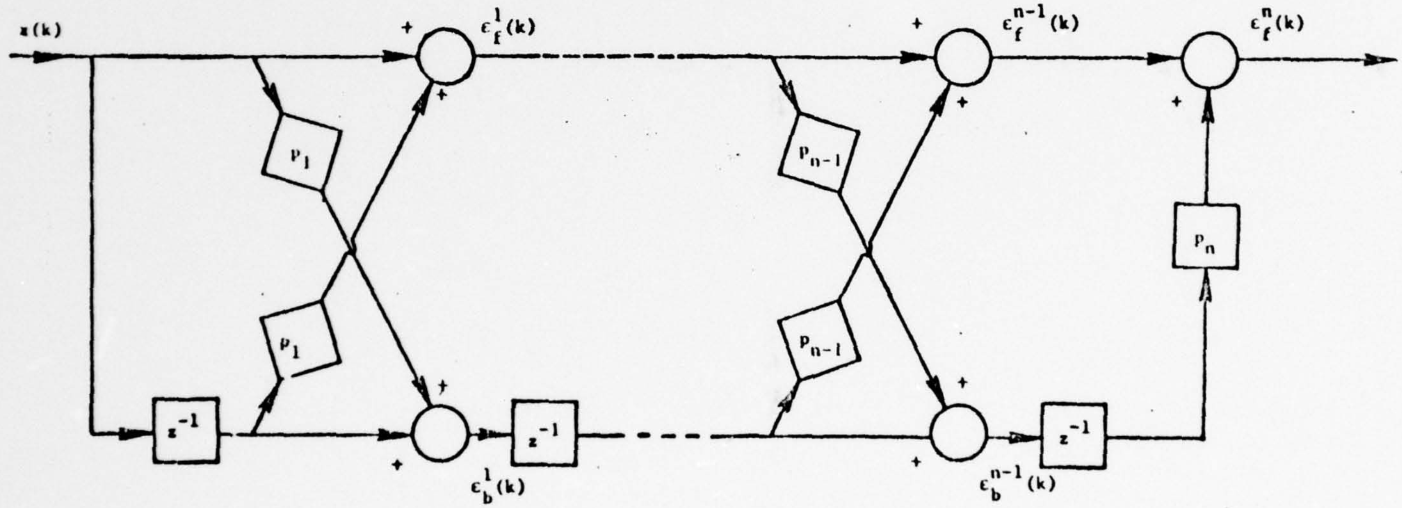

FIG. 2: REALIZATION OF $H(z^{-1})$

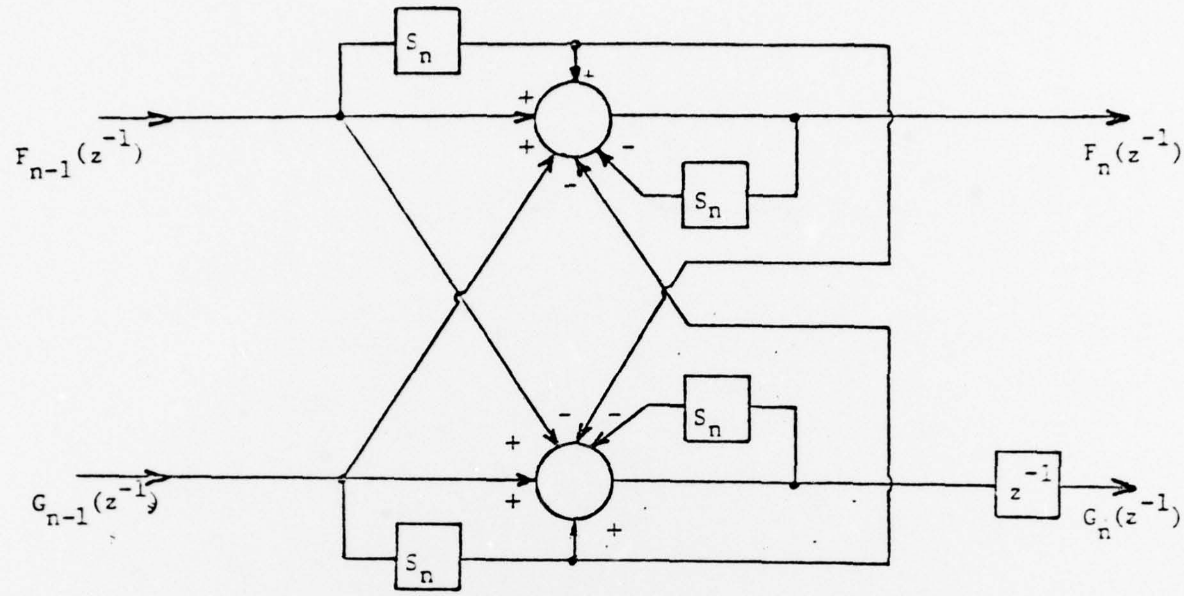

FIG. 3: REALIZATION USING THE PARAMETERS S_n

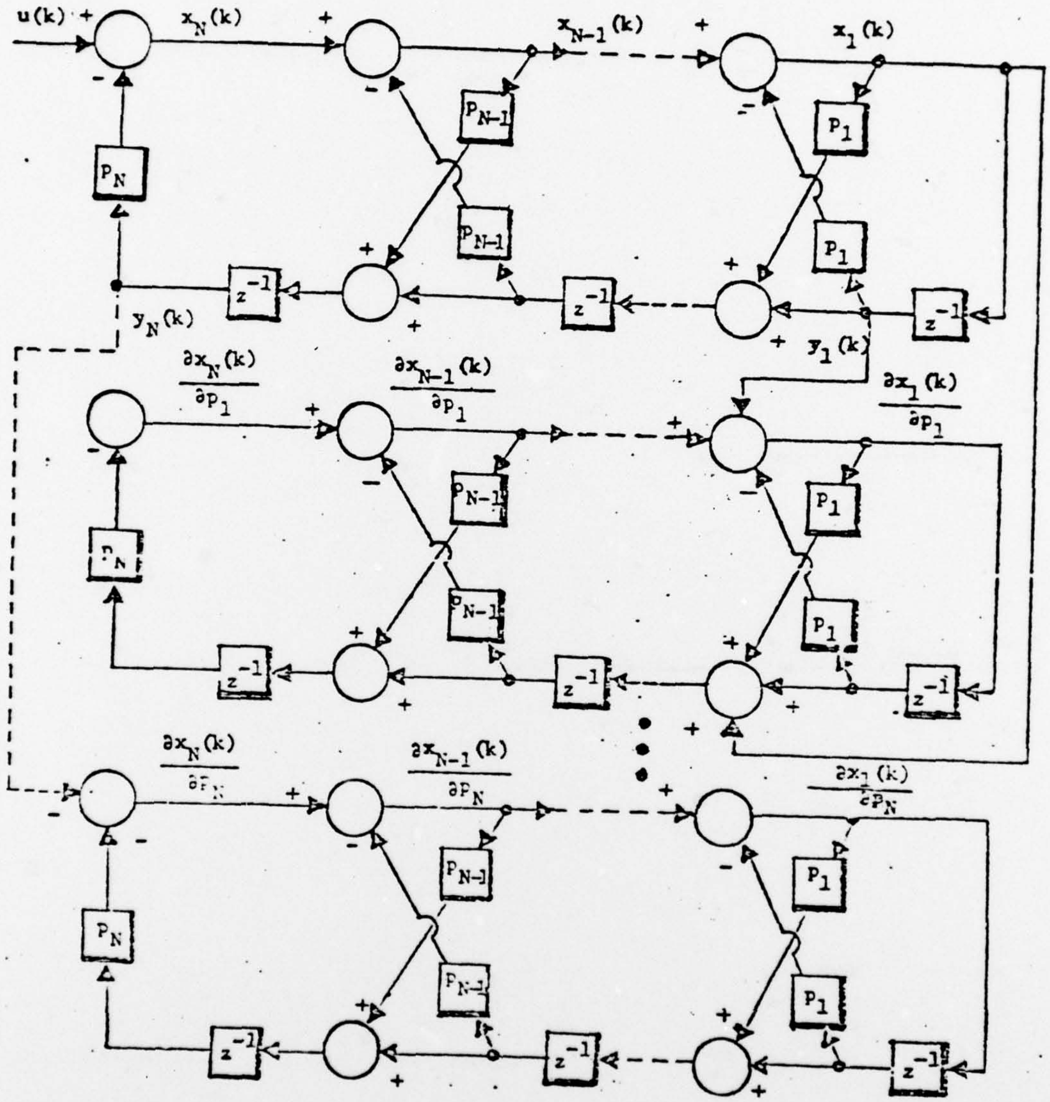

FIG. 4 GENERATION OF SENSITIVITY FUNCTIONS FOR THE LATTICE FORM FILTER REALIZATION

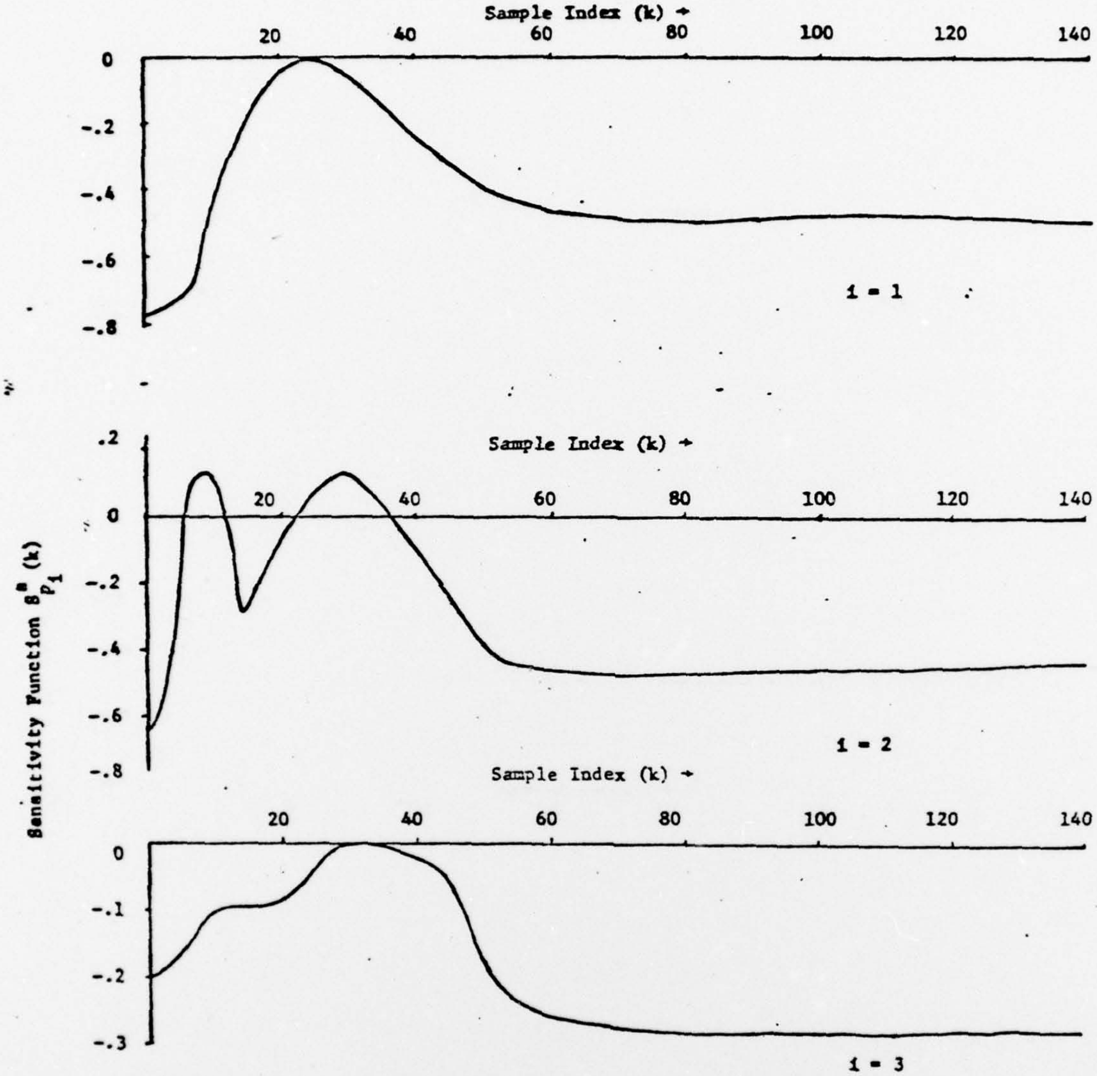

FIG. 5: SENSITIVITY FUNCTIONS OF $\{p_n\}$

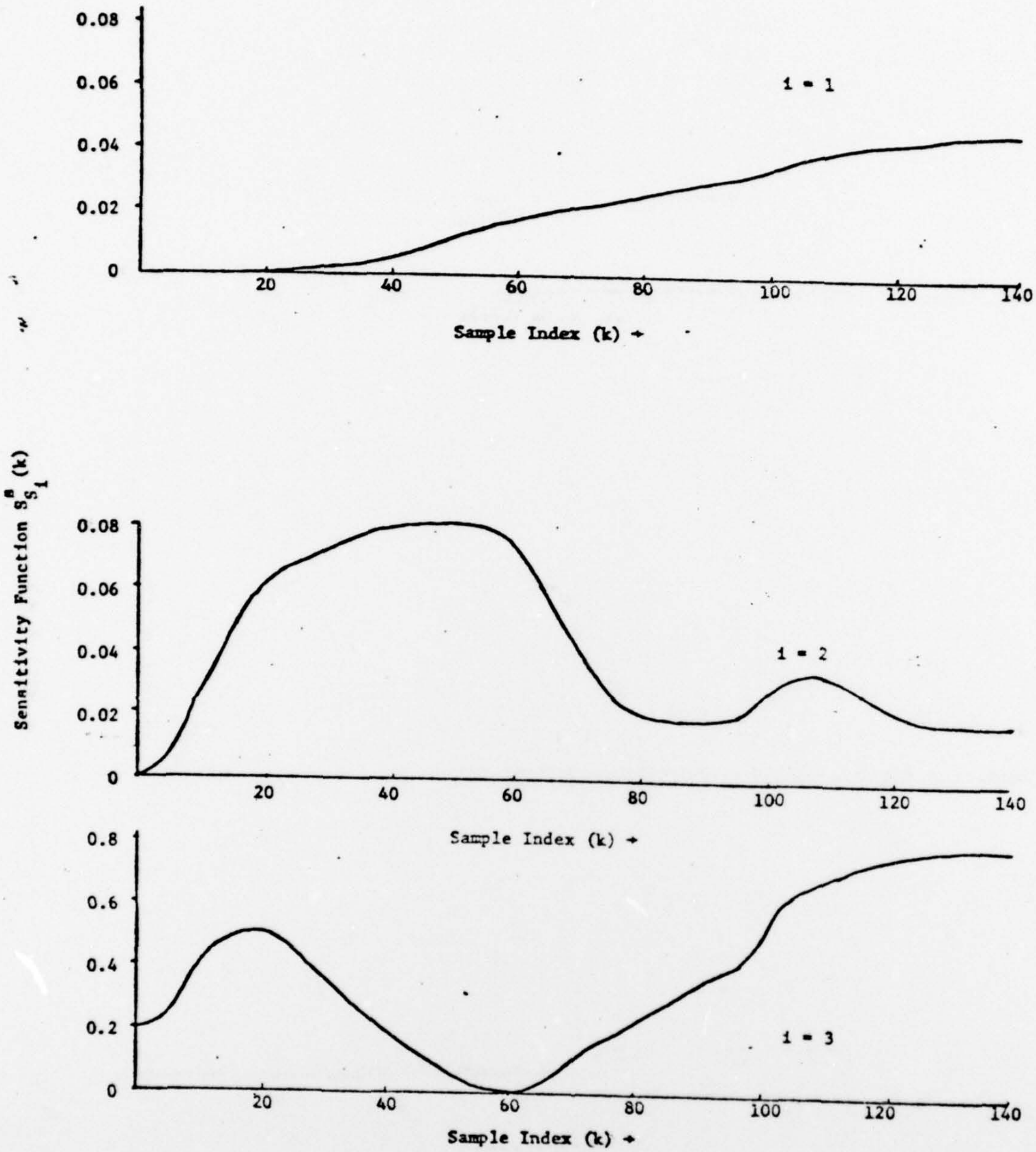

FIG. 6: SENSITIVITY FUNCTIONS OF $\{S_n\}$

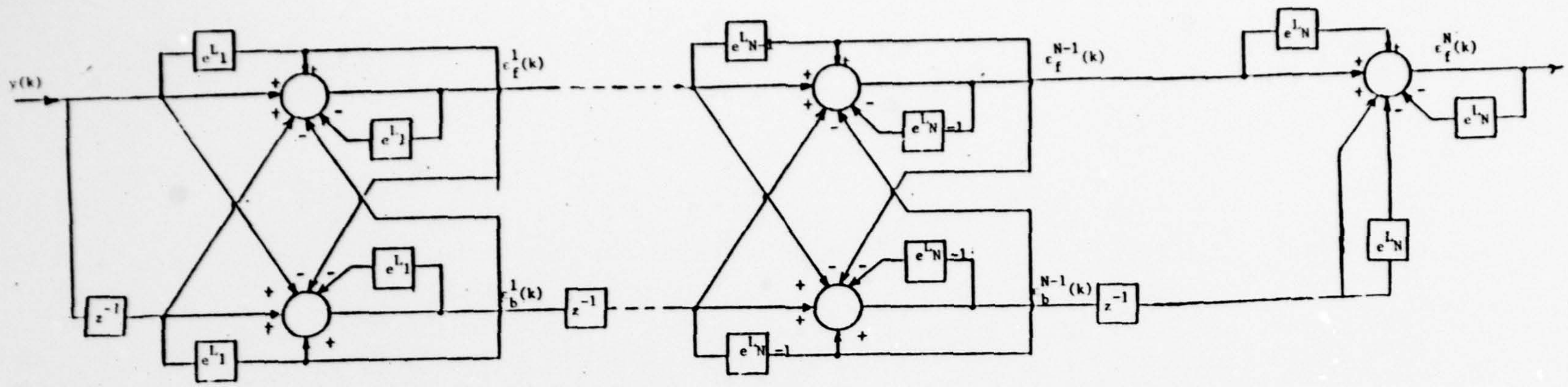

Fig. 7 IDENTIFICATION OF $\{L_n\}$

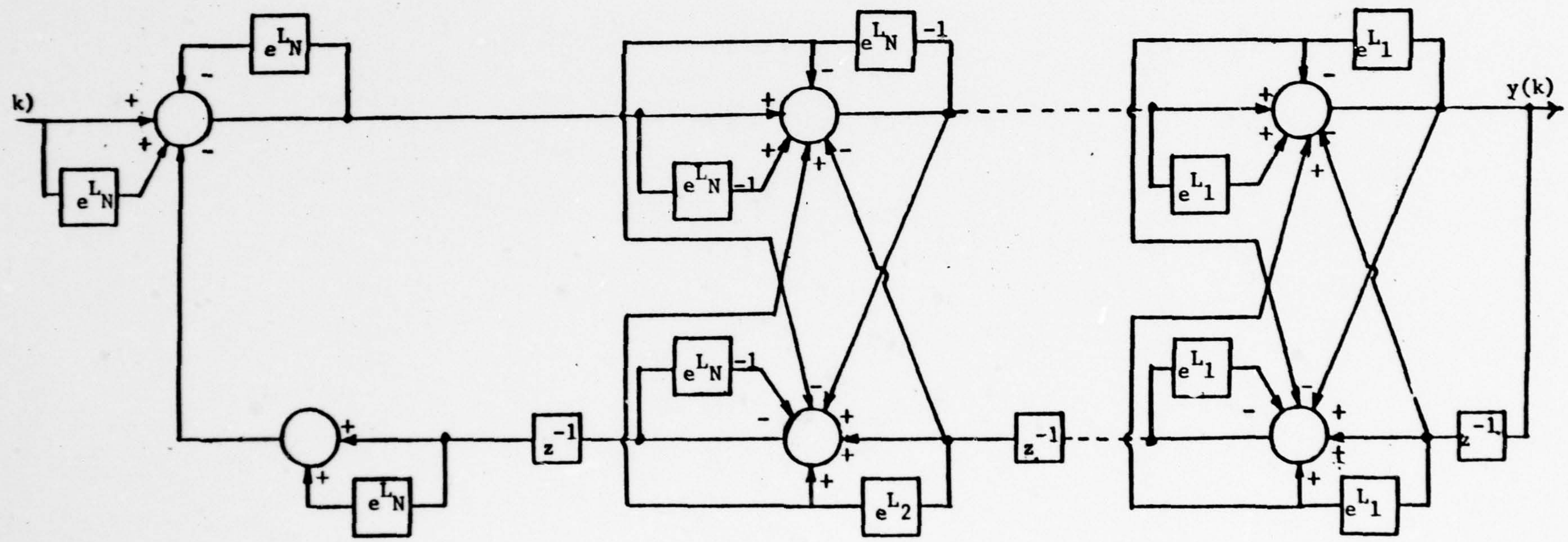

Fig. 8. MODEL FOR GENERATING $y(\cdot)$ USING THE COEFFICIENTS $\{L_n\}$

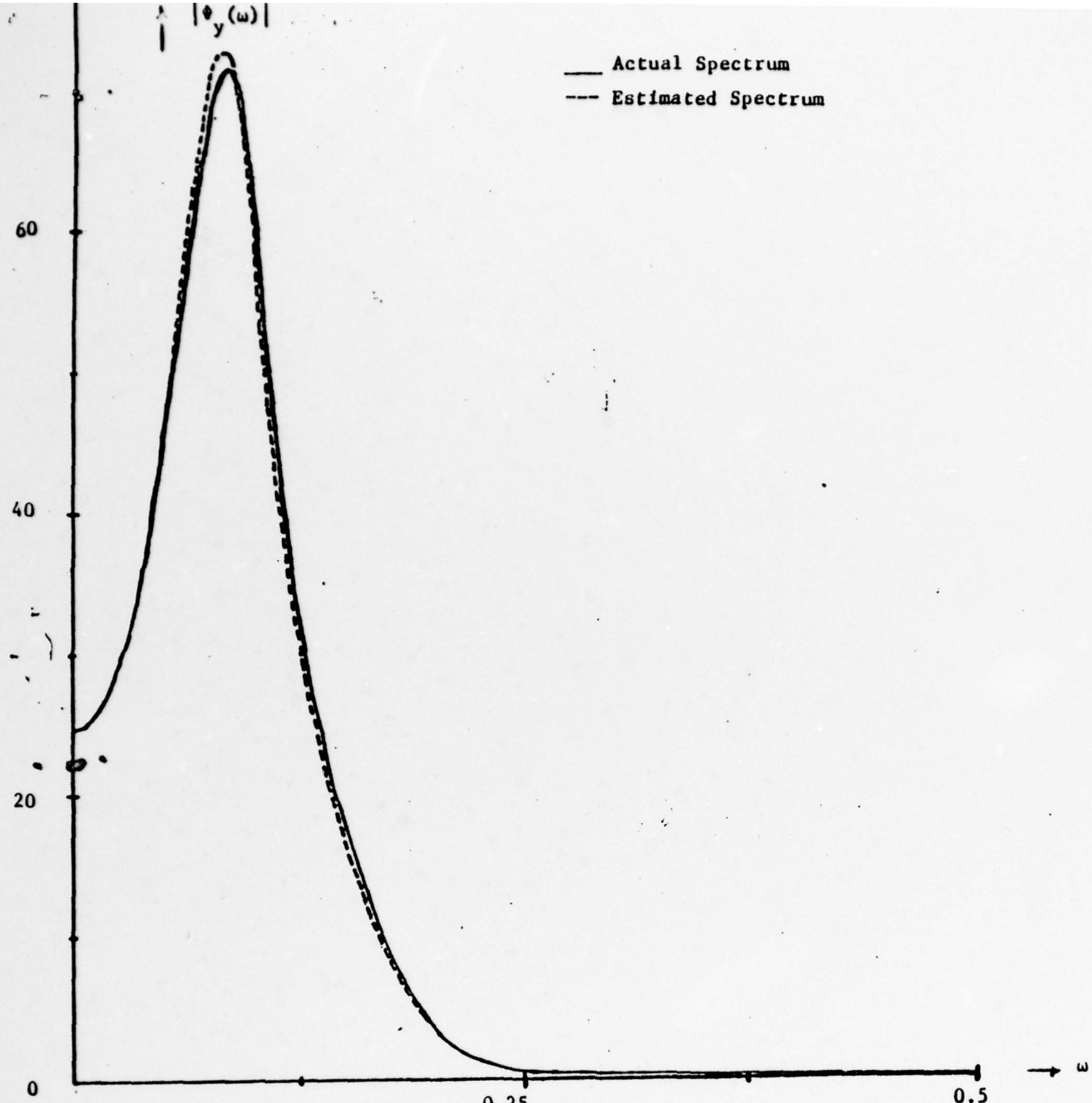

Fig. 9. ACTUAL AND ESTIMATED SPECTRA FOR AN EXAMPLE.

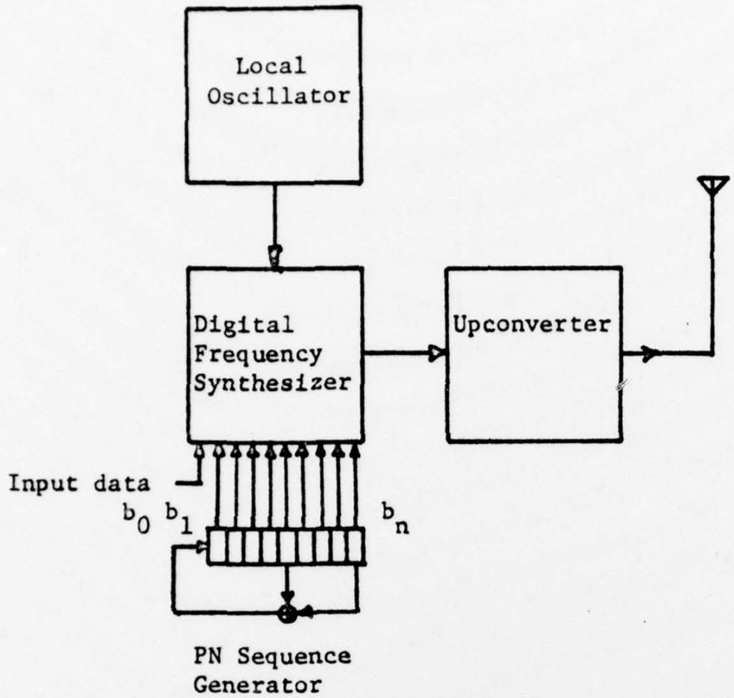

FIG. 10. BLOCK DIAGRAM OF AN FH TRANSMITTER

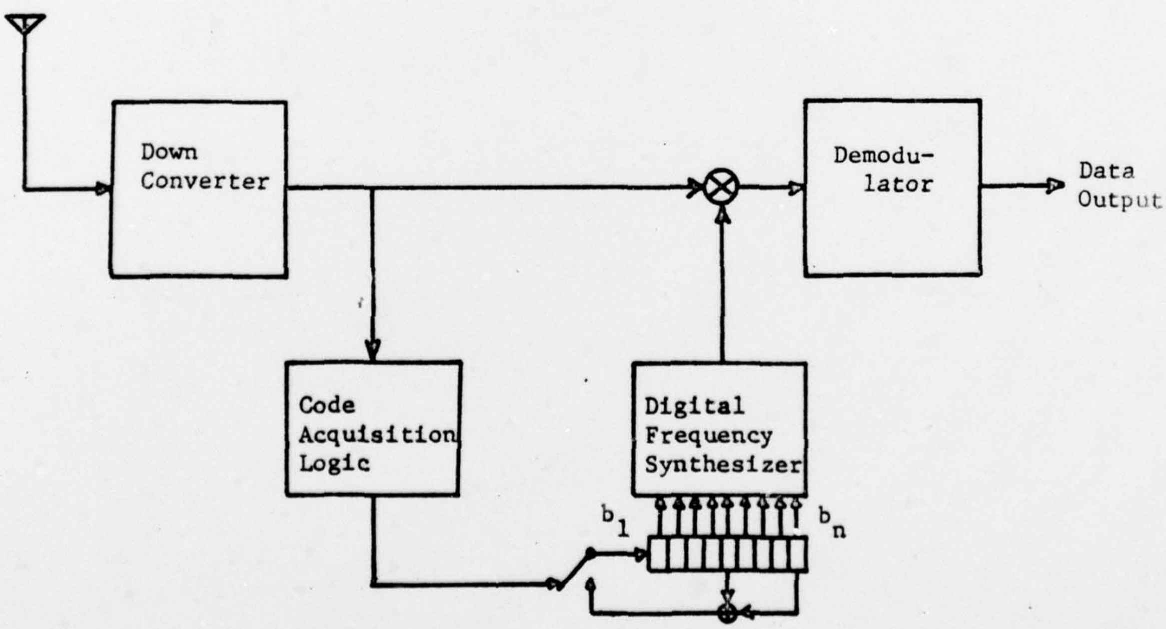

FIG. 11. BLOCK DIAGRAM OF AN FH RECEIVER